Etalon 1054 Measurements

I. History

Etalon 1054 is the high resolution etalon for SALT PFIS. It provides the high spectral resolution mode working with the low resolution etalon in dual-etalon mode. The required characteristics for the etalon were developed in consultation with the SALT Science Working Group and through the PDR process, with input from the vendor, ICOS, about the feasibility of the proposed specifications. The final specifications for the etalon are listed in Table 1. ICOS submitted a quotation for the system on December 12, 2001. The order for this etalon was held in reserve, to provide a contingency fund if early cost over-runs occurred in the PFIS project. At the November, 2002 SALT Science Working Group and Board meetings the procurement of the etalon was approved. The etalon was ordered on December 8, 2002.

Table 1 High Resolution Etalon Specifications

clear aperture	150 mm
surface quality	λ/100 at 650 nm
finesse	approximately 30 at 650 nm
reflector coating	90% ± 4% from 430 nm to 860 nm
spectral resolution	12500 at 650 nm
(implied gap)	135 microns
glass reference capacitor	
outer surface AR coating	<1% from 430nm to 680 nm

Delays in producing the first two PFIS etalons resulted in delays in the completion of etalon 1054. The etalon was received at Rutgers on March 4, 2005. During shipping to SAAO in March 2005, one of the pressure pads failed in a way similar to that of etalon 1052 during initial shipment. The loss of the pressure pad lead to the opening of several of the optical contacts between two of the piezo spacers and the plates and between one of the capacitors and the plates, rendering the etalon inoperable. The etalon was returned to the vendor for repair in April 2005, where it was at the time of this report.

II. Test Results

The testing equipment used for characterizing this etalon is the same as described in the report on etalon 1052. The gap of the high resolution etalon is large compared to the range of motion of the piezo actuators, so no significant variation of the etalon's spectral resolution is possible. We will operate the etalon near its maximum gap setting to attain the highest resolution possible. The Z axis coarse setting of the controller adopted is Zc=+2. The operating mode is named HR (high resolution). The measured properties of the etalon are presented in Table 2. Here and below, we report FWHM, spectral resolution, and transmission profiles after the instrumental profile of the measuring spectrograph has been deconvolved. Measurements in the 420 to 550 nm wavelength range were carried out with a 2400 line/mm grating, which produces an instrumental profile of 0.50 to 0.44Å FWHM over this wavelength range. Measurements at longer wavelengths were done with the 1800 line/mm grating, which produces an instrumental profile of 0.67 to 0.47Å FWHM over the 550 to 900 nm wavelength range.

Table 2 HR Mode Properties

Wave (Å)	FWHM (Å)	FSR (Å)	Finesse	Resolution	Gap (μ)	X offset	Y offset
4216.76	1.74	6.58	3.8	2423	135.1		
4223.34	1.54	6.62	4.3	2742	134.7		
4230.00	1.52	6.65	4.4	2783	134.4		
4236.65	1.34	6.66	5.0	3162	134.9		
4243.31	1.26	6.68	5.3	3368	134.9		
4250.00	1.30	6.69	5.1	3269	135.0		
4256.69	1.35	6.70	5.0	3153	135.3		
4263.39	1.28	6.72	5.3	3331	135.2		
4270.13	1.24	6.76	5.5	3444	134.9		
4276.91	1.27	6.76	5.3	3368	135.2		
4283.66	1.17	6.75	5.8	3661	135.9		
4290.61	1.12	6.81	6.1	3831	135.3		
4297.27	1.06	6.86	6.5	4054	134.6		
4304.13	1.07	6.86	6.4	4023	135.0		
4310.99	0.98	6.88	7.0	4399	135.2		
4317.88	0.97	6.89	7.1	4451	135.2		
4324.78	0.87	6.91	7.9	4971	135.2		
4331.71	0.87	6.95	8.0	4979	135.1		
4338.67	0.81	6.97	8.6	5356	135.0		
4345.65	0.78	6.99	9.0	5571	135.0		
4352.66	0.76	7.02	9.2	5727	134.9		
4359.69	0.71	7.04	9.9	6140	135.0		
4366.74	0.70	7.05	10.1	6238	135.2		
4373.80	0.57	7.10	12.4	7673	134.8		
4380.90	0.54	7.11	13.2	8113	134.9		
4388.03	0.52	7.14	13.7	8439	134.8		
4395.18	0.50	7.17	14.3	8790	134.8		
4402.36	0.50	7.19	14.4	8805	134.8		
4409.55	0.50	7.21	14.4	8819	134.9		
4416.78	0.51	7.24	14.2	8660	134.7		
4424.03	0.51	7.26	14.2	8675	134.7		
4431.30	0.45	7.29	16.2	9847	134.8		
4438.60	0.48	7.31	15.2	9247	134.7		
4445.93	0.46	7.34	16.0	9665	134.7		
4453.28	0.49	7.36	15.0	9088	134.7		
4460.65	0.47	7.39	15.7	9491	134.6		

Wave	FWHM	FSR	Finesse	Resolution	Gap	X offset	Y offset
4468.06	0.50	7.41	14.8	8936	134.6		
4475.48	0.46	7.44	16.2	9729	134.7		
4482.93	0.52	7.47	14.4	8621	134.6		
4490.41	0.48	7.49	15.6	9355	134.6		
4497.91	0.46	7.52	16.3	9778	134.6	30	45
4505.44	0.51	7.54	14.8	8834	134.6		
4513.00	0.48	7.57	15.8	9402	134.5		
4520.58	0.51	7.58	14.9	8864	134.7		
4528.18	0.54	7.64	14.1	8386	134.2		
4535.82	0.55	7.65	13.9	8247	134.5		
4543.48	0.56	7.67	13.7	8113	134.6		
4551.16	0.58	7.70	13.3	7847	134.6		
4558.87	0.58	7.72	13.3	7860	134.5		
4566.61	0.58	7.76	13.4	7873	134.5		
4574.38	0.59	7.79	13.2	7753	134.4		
4582.18	0.60	7.81	13.0	7637	134.4		
4590.00	0.59	7.84	13.3	7780	134.4		
4597.85	0.61	7.86	12.9	7537	134.5		
4605.72	0.62	7.89	12.7	7429	134.4		
4613.63	0.63	7.92	12.6	7323	134.4		
4621.56	0.60	7.95	13.2	7703	134.4		
4629.52	0.61	7.97	13.1	7589	134.4		
4637.51	0.61	8.00	13.1	7602	134.3		
4645.53	0.62	8.03	13.0	7493	134.4		
4653.57	0.61	8.06	13.2	7629	134.3		
4661.65	0.60	8.09	13.5	7769	134.3		
4669.75	0.59	8.12	13.8	7915	134.4		
4677.88	0.60	8.13	13.6	7796	134.6		
4685.91	0.59	8.17	13.8	7942	134.4		
4694.08	0.57	8.18	14.4	8235	134.6		
4702.28	0.57	8.22	14.4	8250	134.6		
4710.51	0.57	8.25	14.5	8264	134.6		
4718.77	0.57	8.27	14.5	8279	134.6		
4727.05	0.57	8.30	14.6	8293	134.6		
4735.37	0.59	8.33	14.1	8026	134.6		
4743.71	0.56	8.34	14.9	8471	134.9		
4752.22	0.53	8.42	15.9	8966	134.1		
4760.64	0.55	8.43	15.3	8656	134.3		
4769.09	0.55	8.46	15.4	8671	134.3		
4777.57	0.57	8.49	14.9	8382	134.3		
4786.08	0.55	8.52	15.5	8702	134.4		
4794.61	0.54	8.55	15.8	8879	134.4		
4803.18	0.54	8.59	15.9	8895	134.4		
4811.78	0.55	8.61	15.7	8749	134.5		

Wave	FWHM	FSR	Finesse	Resolution	Gap	X offset	Y offset
4820.40	0.55	8.64	15.7	8764	134.4		
4829.07	0.55	8.68	15.8	8780	134.3		
4837.76	0.52	8.70	16.7	9303	134.5		
4846.47	0.53	8.73	16.5	9144	134.5		
4855.22	0.54	8.76	16.2	8991	134.5		
4864.00	0.54	8.80	16.3	9007	134.4		
4872.82	0.53	8.83	16.7	9194	134.5		
4881.66	0.53	8.86	16.7	9211	134.5		
4890.54	0.53	8.84	16.7	9227	135.3		
4899.34	0.53	8.87	16.7	9244	135.3		
4908.28	0.53	8.96	16.9	9261	134.4		
4917.26	0.53	9.00	17.0	9278	134.4		
4926.27	0.52	9.03	17.4	9474	134.4		
4935.31	0.51	9.06	17.8	9677	134.4		
4944.39	0.53	9.09	17.2	9329	134.4		
4953.50	0.54	9.13	16.9	9173	134.4		
4962.65	0.53	9.16	17.3	9363	134.4		
4971.83	0.55	9.08	16.5	9040	136.2		
4980.80	0.56	9.24	16.5	8894	134.2		
4990.32	0.57	9.40	16.5	8755	132.5		
4999.60	0.56	9.31	16.6	8928	134.3	25	35
5008.93	0.57	9.34	16.4	8788	134.3		
5018.28	0.58	9.37	16.2	8652	134.4		
5027.67	0.56	9.41	16.8	8978	134.3		
5037.10	0.58	9.45	16.3	8685	134.3		
5046.56	0.56	9.47	16.9	9012	134.4		
5056.05	0.56	9.49	16.9	9029	134.7		
5065.74	0.55	9.57	17.4	9210	134.1		
5075.31	0.59	9.59	16.2	8602	134.4		
5084.91	0.59	9.62	16.3	8618	134.4		
5094.55	0.59	9.66	16.4	8635	134.3		
5104.23	0.58	9.69	16.7	8800	134.4		
5113.94	0.59	9.73	16.5	8668	134.4		
5123.69	0.60	9.77	16.3	8539	134.4		
5133.47	0.61	9.78	16.0	8416	134.7		
5143.23	0.61	9.86	16.2	8432	134.1		
5153.09	0.61	9.88	16.2	8448	134.4		
5162.99	0.60	9.92	16.5	8605	134.4		
5172.93	0.63	9.95	15.8	8211	134.4		
5182.90	0.64	9.99	15.6	8098	134.4		
5192.92	0.64	10.04	15.7	8114	134.4		
5202.97	0.62	10.07	16.2	8392	134.5		
5213.05	0.64	10.08	15.7	8145	134.8		
5223.24	0.64	10.17	15.9	8161	134.1		

Wave	FWHM	FSR	Finesse	Resolution	Gap	X offset	Y offset
5233.41	0.64	10.19	15.9	8177	134.4		
5243.62	0.65	10.23	15.7	8067	134.4		
5253.87	0.65	10.27	15.8	8083	134.4		
5264.16	0.66	10.30	15.6	7976	134.5		
5274.48	0.66	10.32	15.6	7992	134.8		
5284.65	0.64	10.44	16.3	8257	133.8		
5295.09	0.64	10.46	16.3	8274	134.0		
5305.57	0.63	10.50	16.7	8422	134.0		
5316.09	0.64	10.54	16.5	8306	134.1		
5326.64	0.65	10.57	16.3	8195	134.2		
5337.24	0.65	10.61	16.3	8211	134.2		
5347.86	0.65	10.65	16.4	8227	134.3		
5358.53	0.65	10.68	16.4	8244	134.4		
5369.23	0.63	10.72	17.0	8523	134.5		
5379.97	0.64	10.76	16.8	8406	134.6		
5390.74	0.64	10.77	16.8	8423	134.9		
5401.72	0.61	10.88	17.8	8855	134.1		
5412.60	0.63	10.90	17.3	8591	134.4		
5423.51	0.67	10.93	16.3	8095	134.6		
5434.46	0.62	10.98	17.7	8765	134.5		
5445.47	0.65	11.03	17.0	8378	134.5		
5456.51	0.63	11.07	17.6	8661	134.5		
5467.60	0.65	11.11	17.1	8412	134.5		
5478.73	0.65	11.15	17.2	8429	134.5		
5489.91	0.65	11.21	17.2	8446	134.5		
5501.14	0.65	11.24	17.3	8463	134.6	25	45
5512.40	0.67	11.29	16.9	8227	134.6		
5523.72	0.65	11.34	17.4	8498	134.5		
5535.08	0.65	11.36	17.5	8516	134.8		
5546.51	0.58	11.46	19.8	9563	134.2		
5557.97	0.54	11.48	21.3	10293	134.5		
5569.47	0.60	11.53	19.2	9282	134.5		
5581.03	0.60	11.57	19.3	9302	134.6		
5592.61	0.60	11.63	19.4	9321	134.5		
5604.28	0.61	11.68	19.1	9187	134.5		
5615.97	0.61	11.72	19.2	9207	134.6		
5627.71	0.61	11.76	19.3	9226	134.6		
5639.50	0.62	11.81	19.0	9096	134.6		
5651.33	0.63	11.86	18.8	8970	134.6		
5663.22	0.64	11.92	18.6	8849	134.6		
5675.16	0.65	11.95	18.4	8731	134.7		
5687.13	0.64	12.01	18.8	8886	134.7		
5699.17	0.63	12.07	19.2	9046	134.6		
5711.26	0.63	12.11	19.2	9065	134.7		

Wave	FWHM	FSR	Finesse	Resolution	Gap	X offset	Y offset
5723.39	0.64	12.16	19.0	8943	134.7		
5735.58	0.64	12.21	19.1	8962	134.7		
5747.82	0.66	12.24	18.5	8709	135.0		
5760.24	0.71	12.35	17.4	8113	134.3		
5772.59	0.71	12.38	17.4	8130	134.6		
5784.99	0.72	12.42	17.3	8035	134.7		
5797.44	0.73	12.48	17.1	7942	134.7		
5809.95	0.73	12.53	17.2	7959	134.7		
5822.50	0.73	12.58	17.2	7976	134.7		
5835.11	0.75	12.64	16.9	7780	134.7		
5847.78	0.73	12.67	17.4	8011	135.0		
5860.64	0.72	12.77	17.7	8140	134.5		
5873.41	0.74	12.80	17.3	7937	134.8		
5886.24	0.76	12.86	16.9	7745	134.8		
5899.12	0.77	12.91	16.8	7661	134.8		
5912.06	0.78	12.97	16.6	7580	134.8		
5925.05	0.79	13.02	16.5	7500	134.8		
5938.10	0.79	13.08	16.6	7517	134.8		
5951.21	0.78	13.13	16.8	7630	134.8		
5964.37	0.78	13.19	16.9	7647	134.9		
5977.59	0.82	13.25	16.2	7290	134.8		
5990.87	0.80	13.31	16.6	7489	134.8		
6004.21	0.78	13.37	17.1	7698	134.9	-5	60
6017.60	0.78	13.42	17.2	7715	134.9		
6031.05	0.79	13.48	17.1	7634	134.9		
6044.57	0.76	13.52	17.8	7953	135.1		
6058.32	0.80	13.63	17.0	7573	134.6		
6071.95	0.81	13.66	16.9	7496	135.0		
6085.64	0.80	13.72	17.2	7607	135.0		
6099.39	0.79	13.77	17.4	7721	135.0		
6113.19	0.81	13.84	17.1	7547	135.1		
6127.06	0.83	13.90	16.7	7382	135.0		
6140.99	0.81	13.96	17.2	7581	135.1		
6154.98	0.81	13.99	17.3	7599	135.4		
6169.07	0.82	14.10	17.2	7523	135.0		
6183.17	0.82	14.15	17.3	7540	135.1		
6197.36	0.77	14.21	18.5	8049	135.1	-35	70
6211.59	0.79	14.27	18.1	7863	135.2		
6225.89	0.79	14.33	18.1	7881	135.2		
6240.25	0.80	14.39	18.0	7800	135.3		
6254.67	0.81	14.45	17.8	7722	135.3		
6269.16	0.82	14.52	17.7	7645	135.3		
6283.71	0.84	14.55	17.3	7481	135.7		
6299.00	0.85	14.68	17.3	7411	135.1		

Wave	FWHM	FSR	Finesse	Resolution	Gap	X offset	Y offset
6313.68	0.88	14.71	16.7	7175	135.5		
6328.42	0.82	14.77	18.0	7718	135.5		
6343.23	0.99	14.84	15.0	6407	135.5		
6358.11	0.98	14.91	15.2	6488	135.6		
6373.05	0.79	14.97	18.9	8067	135.7		
6388.05	0.79	15.00	19.0	8086	136.0		
6403.35	0.84	15.15	18.0	7623	135.3	-70	100
6418.50	0.83	15.18	18.3	7733	135.7		
6433.71	0.78	15.25	19.6	8248	135.7		
6449.00	0.77	15.32	19.9	8375	135.8		
6464.34	0.76	15.38	20.2	8506	135.9		
6479.76	0.74	15.45	20.9	8756	135.9		
6495.24	0.74	15.52	21.0	8777	135.9		
6510.80	0.75	15.59	20.8	8681	136.0		
6526.42	0.75	15.66	20.9	8702	136.0		
6542.12	0.77	15.70	20.4	8496	136.3		
6558.25	0.76	15.83	20.8	8629	135.9		
6574.08	0.74	15.86	21.4	8884	136.3		
6589.97	0.77	15.93	20.7	8558	136.3		
6605.94	0.75	16.00	21.3	8808	136.3	-113	135
6621.98	0.77	16.08	20.9	8600	136.4		
6638.10	0.79	16.12	20.4	8403	136.7		
6654.66	0.80	16.25	20.3	8318	136.3		
6670.91	0.79	16.29	20.6	8444	136.6		
6687.24	0.79	16.37	20.7	8465	136.6		
6703.64	0.77	16.44	21.4	8706	136.7		
6720.12	0.79	16.50	20.9	8506	136.8		
6736.65	0.81	16.53	20.4	8317	137.3		
6753.69	0.79	16.70	21.1	8549	136.6		
6770.39	0.79	16.74	21.2	8570	137.0		
6787.16	0.82	16.82	20.5	8277	137.0		
6804.02	0.81	16.89	20.9	8400	137.0	-175	170
6820.94	0.83	16.96	20.4	8218	137.2		
6837.94	0.86	17.05	19.8	7951	137.2		
6855.03	0.91	17.13	18.8	7533	137.2		
6872.19	0.96	17.20	17.9	7159	137.3		
6889.43	0.98	17.24	17.6	7030	137.7		
6907.58	0.87	17.41	20.0	7940	137.0		
6924.99	0.84	17.45	20.8	8244	137.4		
6942.48	0.83	17.54	21.1	8364	137.4		
6960.06	0.84	17.62	21.0	8286	137.5		
6977.72	0.83	17.70	21.3	8407	137.5		
6995.46	0.84	17.78	21.2	8328	137.6	-215	205
7013.29	0.85	17.88	21.0	8251	137.6		

Wave	FWHM	FSR	Finesse	Resolution	Gap	X offset	Y offset
7031.21	0.85	17.97	21.1	8272	137.6		
7049.23	0.86	18.02	21.0	8197	137.9		
7067.27	0.85	18.24	21.5	8314	136.9		
7085.51	0.87	18.27	21.0	8144	137.4		
7103.81	0.88	18.35	20.9	8073	137.5		
7122.21	0.88	18.44	21.0	8093	137.5		
7140.69	0.87	18.53	21.3	8208	137.6		
7159.27	0.92	18.62	20.2	7782	137.6		
7177.93	0.91	18.71	20.6	7888	137.7		
7196.69	0.92	18.80	20.4	7822	137.7	-220	210
7215.54	0.93	18.85	20.3	7759	138.1		
7234.10	1.00	19.07	19.1	7234	137.2		
7253.17	0.98	19.12	19.5	7401	137.6		
7272.34	0.97	19.22	19.8	7497	137.6		
7291.61	0.99	19.32	19.5	7365	137.6		
7310.99	0.95	19.43	20.5	7696	137.5		
7330.48	0.96	19.54	20.4	7636	137.5		
7350.07	0.93	19.65	21.1	7903	137.5		
7369.78	0.93	19.77	21.3	7924	137.4		
7389.61	0.92	19.83	21.6	8032	137.7		
7409.34	1.01	20.05	19.9	7336	136.9		
7429.39	1.02	20.10	19.7	7284	137.3		
7449.54	0.98	20.21	20.6	7602	137.3		
7469.82	0.98	20.34	20.8	7622	137.2		
7490.21	0.96	20.45	21.3	7802	137.1		
7510.73	0.95	20.52	21.6	7906	137.5	-185	195
7531.32	0.98	20.73	21.2	7685	136.8		
7552.05	0.98	20.79	21.2	7706	137.2		
7572.90	0.99	20.90	21.1	7649	137.2		
7593.84	1.00	21.02	21.0	7594	137.2		
7614.94	1.01	21.15	20.9	7540	137.1		
7636.14	1.00	21.27	21.3	7636	137.1		
7657.47	0.99	21.39	21.6	7735	137.1		
7678.92	0.99	21.45	21.7	7756	137.4		
7700.85	0.90	21.66	24.1	8557	136.9		
7722.24	0.97	21.77	22.4	7961	137.0		
7744.01	0.98	21.85	22.3	7902	137.3		
7765.93	0.99	21.99	22.2	7844	137.1		
7788.00	1.02	22.15	21.7	7635	136.9		
7810.22	1.03	22.22	21.6	7583	137.3		
7832.49	0.97	22.40	23.1	8075	136.9		
7854.89	0.98	22.47	22.9	8015	137.3		
7877.44	0.99	22.61	22.8	7957	137.2		
7900.12	1.00	22.76	22.8	7900	137.1		

Wave	FWHM	FSR	Finesse	Resolution	Gap	X offset	Y offset
7922.95	1.01	22.90	22.7	7845	137.1		
7945.91	1.01	23.04	22.8	7867	137.0		
7969.03	1.03	23.12	22.4	7737	137.3		
7992.09	1.02	23.36	22.9	7835	136.7	-170	185
8015.45	1.07	23.43	21.9	7491	137.1		
8038.96	1.11	23.57	21.2	7242	137.1		
8062.59	1.09	23.70	21.7	7397	137.2		
8086.35	1.11	23.85	21.5	7285	137.1		
8110.29	1.13	23.94	21.2	7177	137.4		
8134.43	1.13	24.19	21.4	7199	136.8		
8158.62	1.19	24.26	20.4	6856	137.2		
8182.96	1.19	24.42	20.5	6876	137.1		
8207.45	1.20	24.49	20.4	6840	137.5		
8232.15	1.16	24.79	21.4	7097	136.7		
8256.94	1.17	24.86	21.2	7057	137.1		
8281.87	1.20	25.01	20.8	6902	137.2		
8306.95	1.25	25.08	20.1	6646	137.6		
8332.14	1.25	25.41	20.3	6666	136.6		
8357.55	1.29	25.49	19.8	6479	137.0		
8383.11	1.27	25.62	20.2	6601	137.2		
8408.79	1.33	25.76	19.4	6322	137.2		
8434.64	1.28	25.93	20.3	6590	137.2		
8460.65	1.31	26.01	19.9	6459	137.6		
8486.96	1.33	26.36	19.8	6381	136.6		
8513.32	1.34	26.51	19.8	6353	136.7	-175	200
8539.83	1.36	26.67	19.6	6279	136.7		
8566.50	1.45	26.67	18.4	5908	137.6		
8593.17	1.47	27.02	18.4	5846	136.6		
8620.19	1.50	27.21	18.1	5747	136.5		
8647.40	1.47	27.39	18.6	5883	136.5		
8674.79	1.57	27.57	17.6	5525	136.5		
8702.36	1.47	27.57	18.8	5920	137.3		
8730.25	1.44	27.91	19.4	6063	136.5		
8758.16	1.45	28.07	19.4	6040	136.6		
8786.23	1.52	28.30	18.6	5780	136.4		
8814.53	1.53	28.46	18.6	5761	136.5		
8842.99	1.47	28.46	19.4	6016	137.4		
8870.74	1.65	29.01	17.6	5376	135.6		
8899.75	1.67	29.01	17.4	5329	136.5		
8928.88	1.67	29.27	17.5	5347	136.2		
8958.15	1.69	29.36	17.4	5301	136.7		
8987.59	1.69	29.53	17.5	5318	136.7		
9017.22	1.69	29.63	17.5	5336	137.2	-150	170

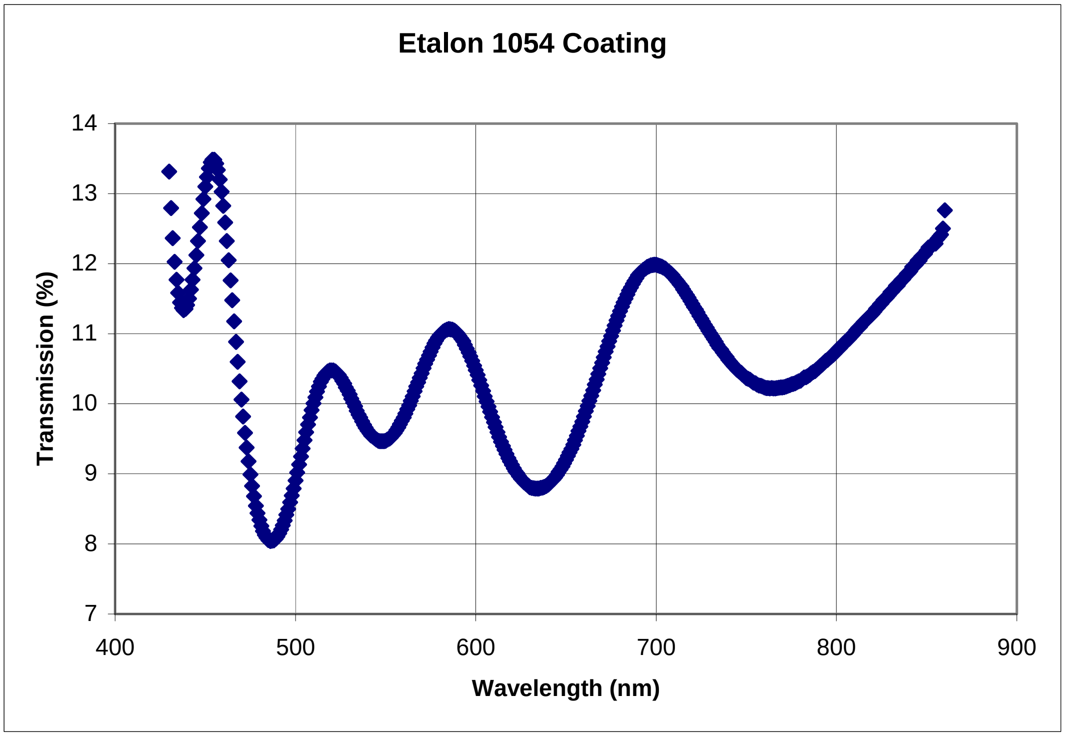

Figure 1 High reflection coating transmission

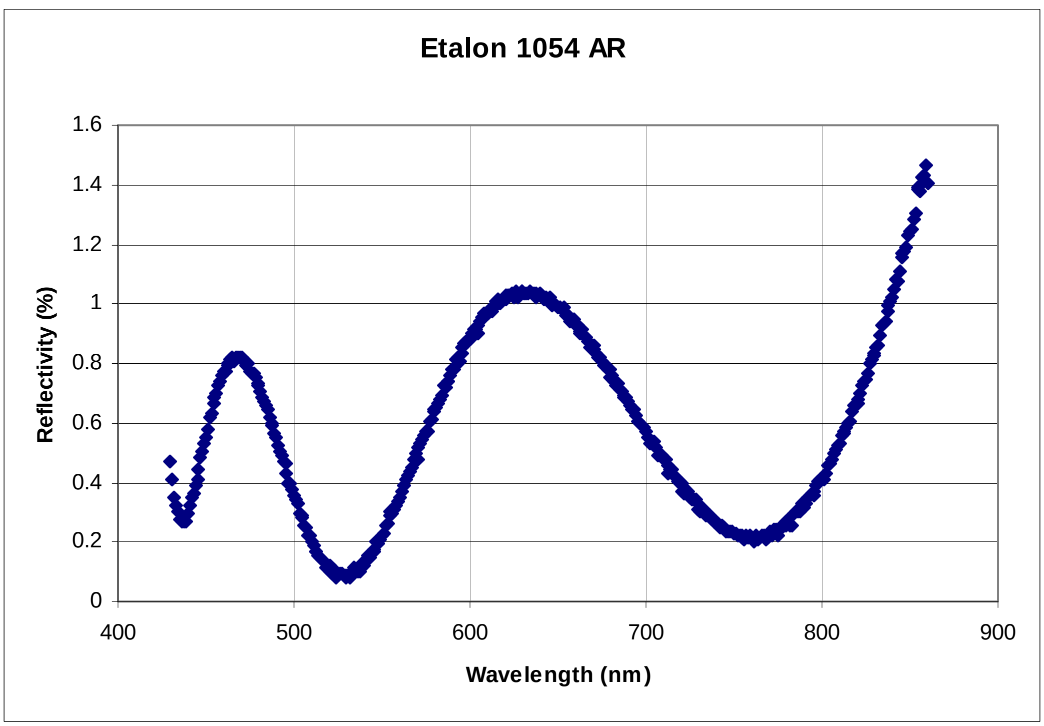

Figure 2 Outer Plate Anti-Reflection Coating

A. Coatings

We do not have facilities to test the reflector coatings or the AR coatings at Rutgers, and show here the curves supplied by ICOS. The high reflector coating curve (Figure 1) shows that the reflector coatings provide 90 +2–3.5 % (peak-to peak) reflectivity over the operating wavelength range, better than the specification. The AR coatings of the outer surfaces of the plates (Figure 2) provide ≤ 1% reflectivity over most of the wavelength range, exceeding the specification slightly from 830 to 860 nm. We do not deem this small failure to meet specification significant, and it should not have an appreciable effect on the system efficiency.

B. Free Spectral Range

The free spectral range (FSR) is the spacing between successive transmission peaks of the Fabry-Perot. The FSR is measured by illuminating the etalon with white light, recording the transmitted spectrum, and measuring the wavelengths of the peaks. There are 315 orders in the specified operating range (430 – 860 nm) in HR mode, and 330 orders in the usable range (430 – 902 nm). The FSR measurements are presented in Table 2 above, and shown in Figure 3. In an ideal etalon, the FSR should vary as the square of the wavelength when the gap is held constant. The barely-visible inflection in the FSR between 6200 and 7200 Å indicates that the effective gap changes in this region (see section C below). The curves in Figure 3 are the expected FSR of an ideal etalon for gaps of 134.5 (red curve) and 137.2 microns (green curve).

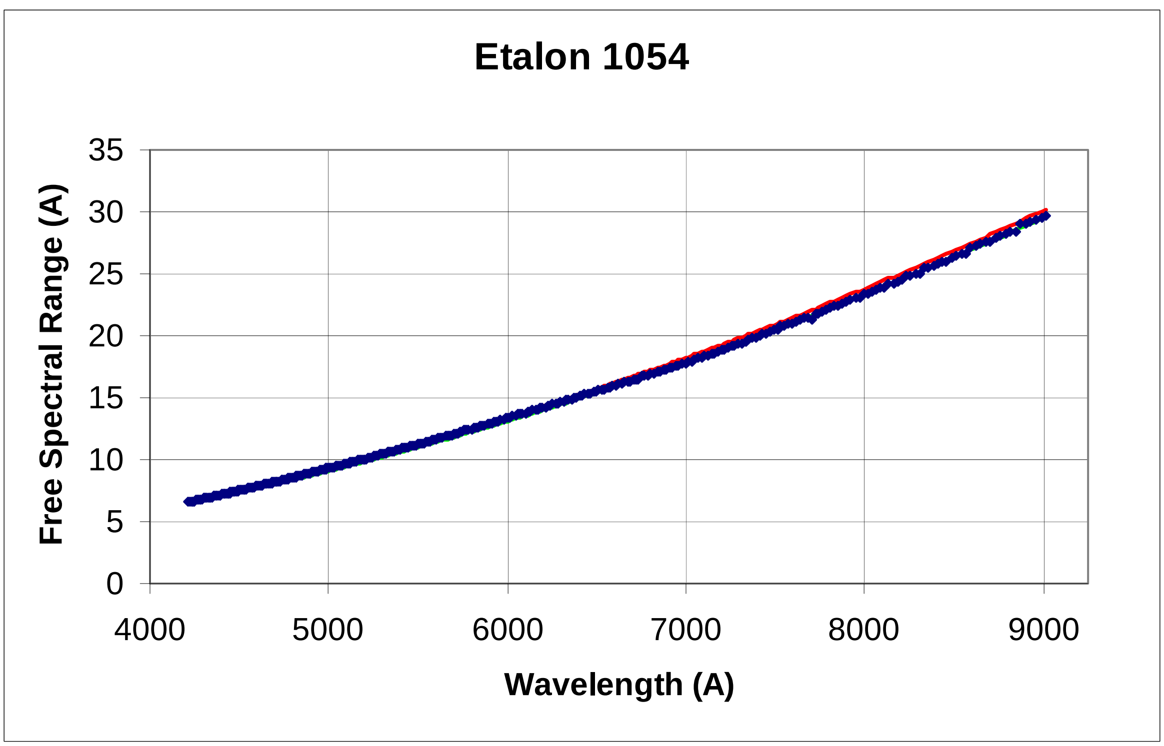

Figure 3 Free Spectral Range in HR Mode

C. Effective Gap and Parallelism

The gap between the reflecting plates is equal to λ^2 / (2 FSR). The gap calculated from our measurements is listed in Table 2 and shown in Figure 4. The effective gap is nearly constant (as expected) at short wavelengths, then increases in the 600 to 710 nm range, and then is roughly constant again at a larger value at long wavelengths. The gap at 650 nm is 135.9 microns, well within the 135±3 micron tolerance of the specifications. This behavior of the effective gap is very similar to that measured for the other PFIS etalons, and arises from the design of the broad band high reflectance coatings. The outlier points in Figure 4 arise from the combination of the sensitivity of the calculation to small wavelength errors and the slight mis-matches in wavelength solutions at the ends of measurement spectra.

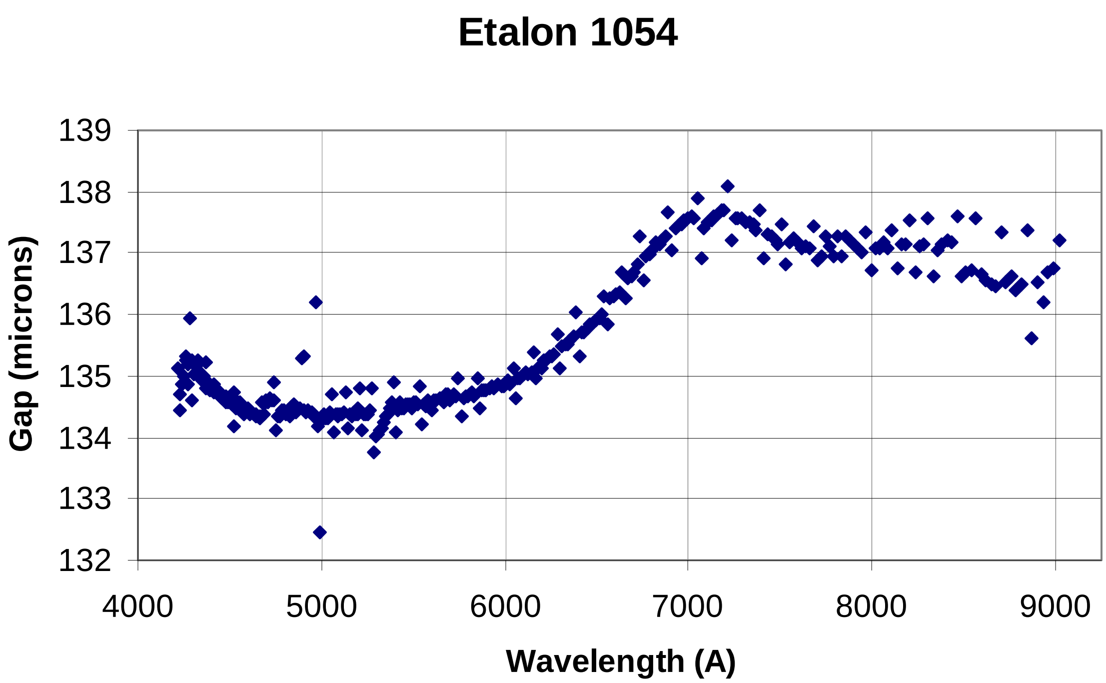

Figure 4 Effective Gap in HR Mode

There is a parallelism effect related to the coating variations. The X and Y motions of the controller adjust the parallelism of the etalon plates. The optimum settings of the parallelism result in the narrowest FWHM and most symmetric spectral profiles of the etalon's transmission. These optimum settings are listed in the "X offset" and "Y offset" columns in Tables 2, and shown in Figure 5. According to ICOS' calibration, 1 offset unit corresponds to 4.9 Å of plate motion. The character of the parallelism adjustments is the same as that of the gap variation: nearly constant at short and long wavelengths, and varying in the 6000 – 7500 Å range. The shape and amplitude of the parallelism variations for this etalon are very similar to those for the other PFIS etalons.

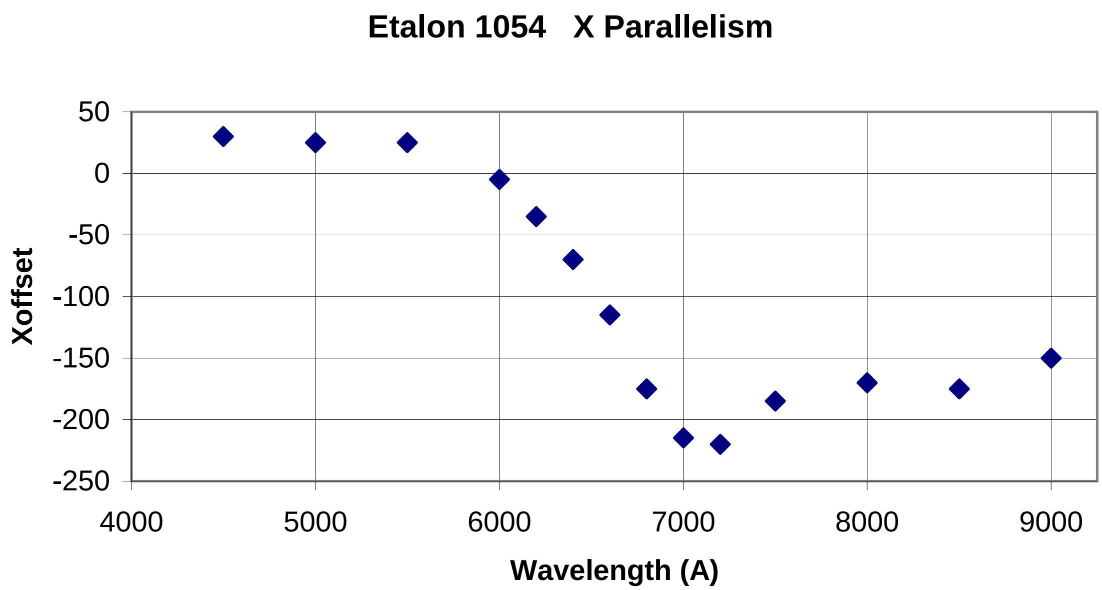

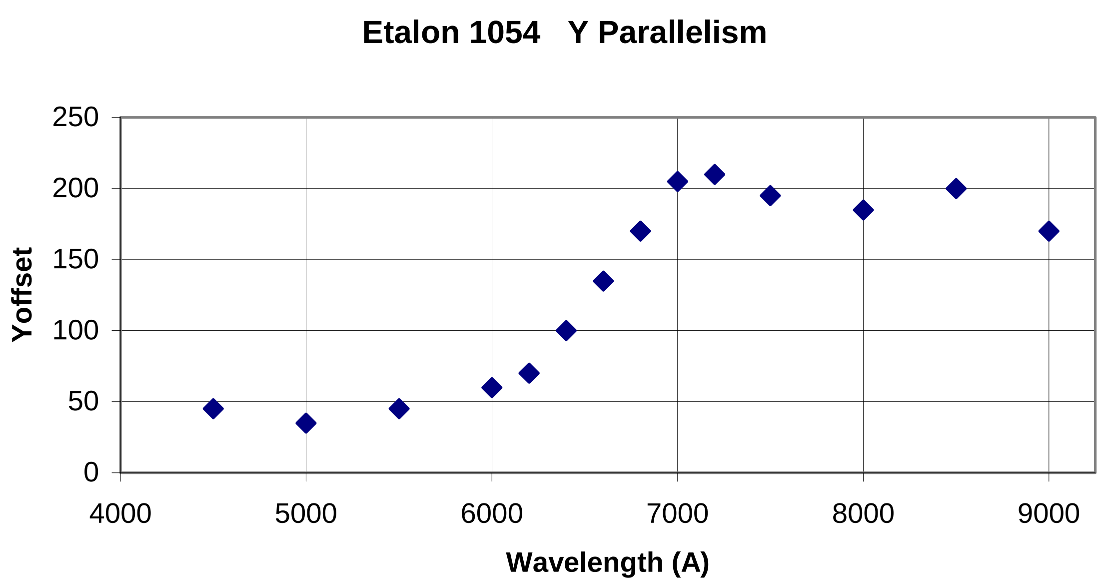

Figure 5 Parallelism Settings in HR Mode

D. Plate Flatness

We have measured the shape of the coated etalon plates by reducing the illuminating aperture in the collimated beam to 25 mm diameter, and then measuring the peak of the transmission profile at each of seven places equally spaced along the Y axis of the etalon; we then rotate the etalon 90˚ and take the same measurements along the X axis. The measurements were made at three wavelengths in HR mode. The effective gap at each position is calculated from the measured wavelength using the relation $D = n \lambda / 2$, where D is the gap and the effective order, n, is calculated from the data in Table 2. The variation of this gap from its central value measures the plate flatness. The results are listed in Table 3 and plotted in Figure 6. As with the other etalons, although the plates were tipped by typically 500 Å in both the X and Y axes to maintain the parallelism over this wavelength range, the measured gaps agree to within ±38 Å. Thus we seem to be mostly measuring the underlying plate shape, after correcting for the coating effects. There are some coating effects, however, since the plates seem to be consistently flatter at the longest wavelength. The plates are very flat in the Y direction, and have a roughly spherical shape in the X direction. The RMS deviation of the plates is 114.8 Å at 6600 Å, or λ/57. Weighting by the area of annular sectors, the weighted RMS deviation is 132.4 Å, or λ/50. The maximum deviation is 223 Å or λ/30. By all of these measures, the plates do not meet the flatness specification of λ/100; this larger than specified plate curvature is responsible for the lower than expected spectral resolution (see Section E below). The fwhm of the profile is somewhat narrower in these restricted apertures than averaged over the entire etalon surface, as expected with the observed large-scale departures from flatness.

Table 3 Etalon 1054 Plate Flatness

Pos.	5000			6600			7900		
	λ	fwhm	Δ Gap	λ	fwhm	Δ Gap	λ	fwhm	Δ Gap
(mm)	(Å)	(Å)	(Å)	(Å)	(Å)	(Å)	(Å)	(Å)	(Å)
X									
-62.5	4999.49	0.49	-265.2	6589.71	0.92	-223.0	7900.19	1.00	-151.0
-50.0	4999.68	0.45	-213.0	6590.00	0.73	-161.7	7900.52	0.91	-95.1
-25.0	5000.07	0.53	-109.5	6590.42	0.90	-74.8	7900.81	1.00	-44.1
0.0	5000.48	0.57	0.0	6590.79	0.86	0.0	7901.06	1.02	0.0
25.0	5000.33	0.56	-39.6	6590.63	0.86	-31.9	7900.91	1.09	-26.6
50.0	4999.98	0.56	-133.0	6590.10	0.89	-142.1	7900.57	1.08	-86.4
62.5	4999.77	0.50	-190.0	6589.81	0.62	-202.7	7900.31	0.94	-131.1
Y									
-62.5	5000.10	0.67	-51.1	6589.64	0.91	-56.3	7899.94	1.15	19.1
-45.0	5000.19	0.69	-26.8	6589.58	0.87	-69.4	7899.77	1.06	-9.4
-20.0	5000.29	0.60	0.5	6589.59	0.57	-66.1	7899.68	0.88	-26.0
0.0	5000.29	0.53	0.0	6589.91	0.52	0.0	7899.83	0.89	0.0
30.0	5000.31	0.56	5.1	6589.79	0.48	-24.6	7899.76	0.88	-11.3
55.0	5000.15	0.67	-36.7	6589.61	0.59	-63.2	7899.75	0.85	-13.4
62.5	4999.91	0.42	-101.4	6589.42	0.53	-102.3	7899.76	0.94	-10.9

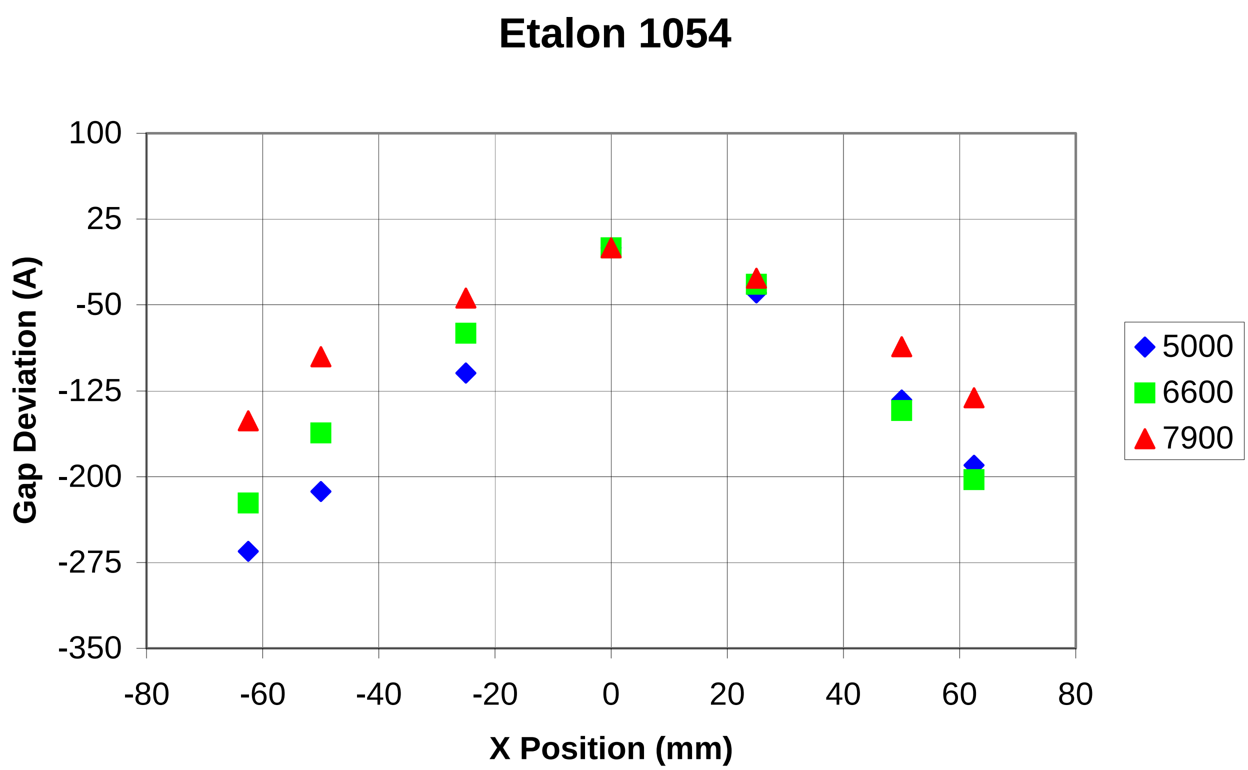

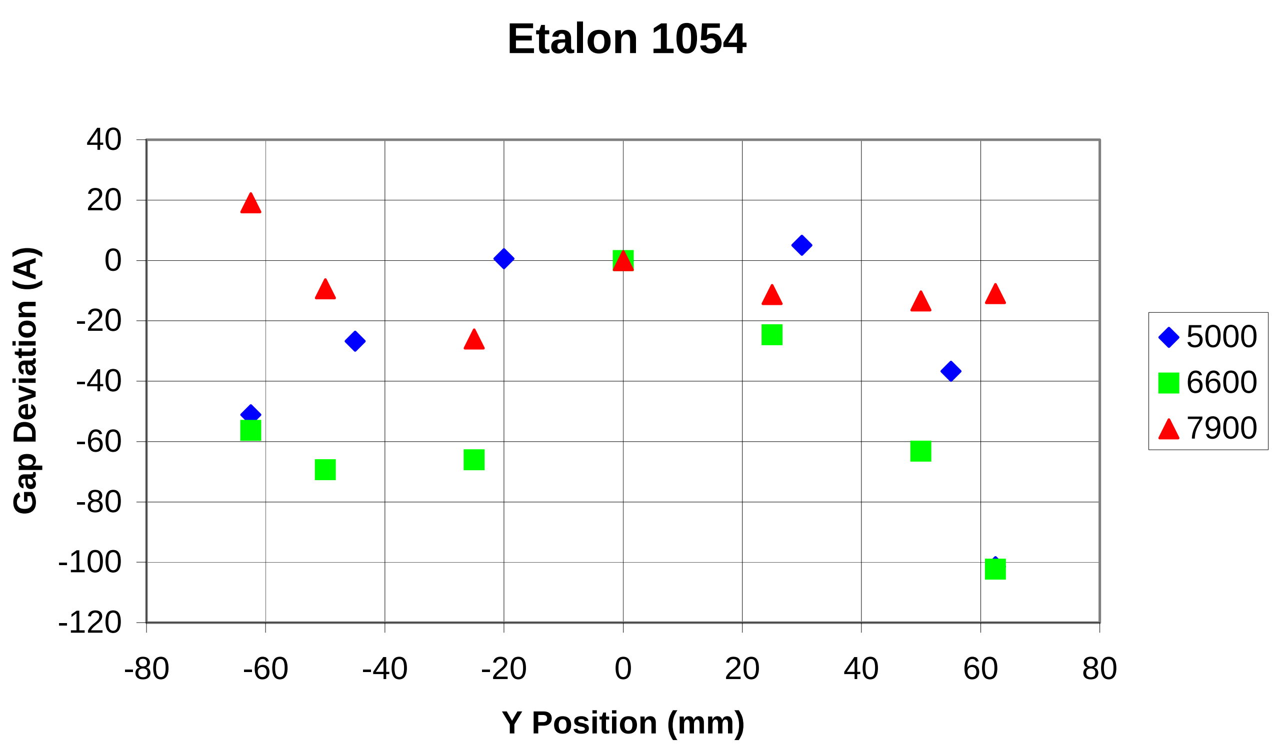

Figure 6 Etalon 1054 Plate Flatness

E. Spectral Resolution

When adjusted for optimum parallelism, the transmission spectral profile of the etalon is well fit by a Voigt function; Figure 7 shows a sample fit. The green curve shows the Voigt fit to the data; the red curve shows the profile after deconvolution of the spectrograph instrumental profile. The FWHM of the Voigt fits is listed in Table 2, and the spectral resolution (λ/FWHM) is listed there and plotted in Figure 8. The resolution at 6542 Å is 8496, less than the specification of 12500. Because of the plate non-flatness, the resolution at all wavelengths is less than desired.

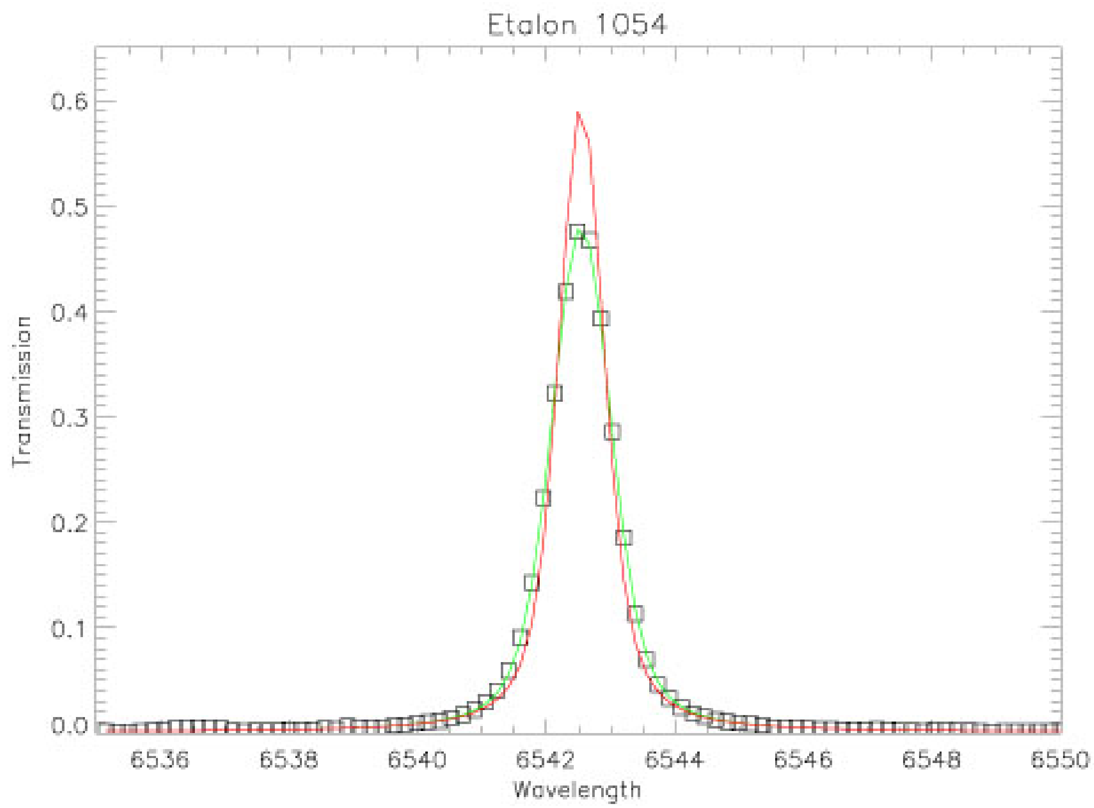

Figure 7 HR Mode Spectral Profile

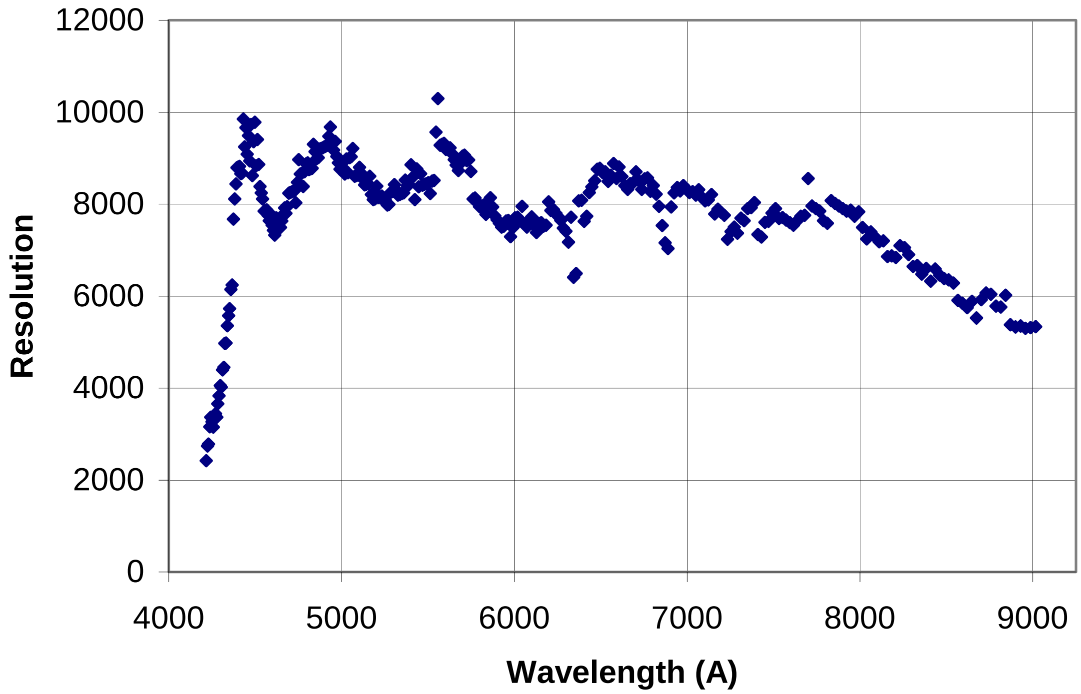

Figure 8 Spectral Resolution in HR Mode

F. Finesse

The finesse is the ratio of the FSR to the FWHM, and is listed in Table 2 and plotted in Figure 9. The finesse at 6542 Å is 20.4, less than the specification of 30. The expected finesse of an etalon depends on the reflectivity of the high reflection coatings and the flatness of the plates. The "reflectivity finesse" is $N_r = \pi R^{1/2} / (1 - R)$ where R is the reflectivity; for our design reflectivity of 90%, $N_r = 30$. The "defect finesse" is $N_d = m / 2$ where m is the plate flatness in waves (λ / m). The total finesse is then $N = (N_r^{-2} + N_d^{-2})^{-1/2}$. Calculating the expected finesse using the above formula with the reflectivity from Figure 1 and the weighted RMS flatness of $\lambda/50$ at 6600 Å from Section D yields the red curve in Figure 9. Treating the plate flatness parameter as a variable, and fitting to obtain the best agreement with the measured finesse curve yields a value of $\lambda/52$ at 6600 Å, producing the green curve in Figure 9. The variations in reflectivity approximately reproduce the shape of the finesse curve, but the fits are not good above 570 nm. This analysis does not account for the variation of plate flatness with wavelength pointed out in Section D, which would improve the finesse at longer wavelengths, as the data suggest.

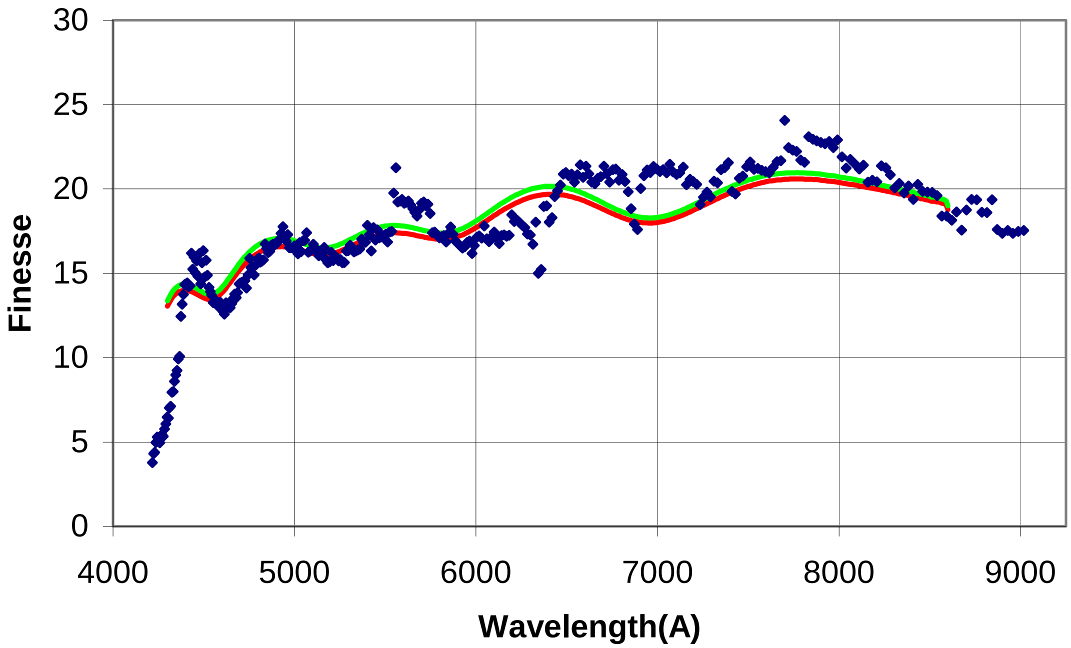

Figure 9 Finesse in HR Mode

G. Transmission

The transmission is measured by taking a spectrum through the etalon, and then sliding the etalon holder to its second position, with an identical aperture, but without the etalon, and taking another spectrum. The ratio of these spectra provides the transmission profile. The power supply to the lamp is highly regulated so the temporal variation of the source brightness is negligible; this was confirmed by repeated cycles of the above measurements. Since the observed line profile is a convolution of the etalon line profile and the spectrograph instrumental profile, the observed peak transmission is lower that the actual peak transmission of the etalon. We deconvolve the instrumental profile, which is well fit by a Gaussian, from the Voigt profile of the etalon to estimate the actual etalon transmission. A sample transmission profile is shown in Figure 7; the green curve is the Voigt fit to the observed profile, and the red curve is the deconvolved Voigt profile. The measured peak transmissions at selected wavelengths are listed in Table 4.

Table 4 Peak Transmission

λ (Å)	T_{meas} (%)	T_{actual} (%)	λ (Å)	T_{meas} (%)	T_{actual} (%)
4506	42	68	7014	64	78
5009	30	49	7511	62	71
5512	36	51	8015	67	75
6031	50	66	8513	65	69
6558	48	59	8988	59	61

H. Wavelength Calibration

The etalon is scanned in wavelength by changing the Z_{offset} in the controller. The scanning range (-2.048 to +2.047 in Z_{offset}) is sufficient to cover several free spectral ranges of the etalon. Since the change of the gap during scanning is a relatively small fraction of the gap (about 1.5% maximum), the spectral resolution is not significantly changed over the full scanning range. To simplify operation, we have decided to operate the etalon in the minimum number of orders (54) that will allow scanning to any wavelength within the operating range (430 – 900 nm). The results are presented in Table 5. Columns 1-4 contain the coefficients of the polynomial fit $\lambda = A + B Z' + C Z'^2 + D Z'^3$ where $Z' = Z_{offset} / 1000$. Column 5 has the RMS scatter of the measurements about this fit. The polynomials provide excellent fits, with residuals less than 1/40 of the FWHM. We expect that the B, C and D coefficient values measured here should be very stable, but that the A coefficient value will vary with time, temperature, humidity and other environmental factors (see section I).

Table 5 Wavelength Scanning Calibration

A	B	C	D	Δλ (Å)
4290.440	16.713833	0.011497	0.006252	0.018
4352.611	16.965651	0.020019	0.006266	0.020
4416.784	17.235980	0.009266	0.006172	0.013
4475.436	17.495631	0.009203	0.006103	0.012
4535.770	17.759311	0.008537	0.005484	0.014
4597.755	17.980750	0.013501	0.007410	0.021
4661.534	18.274270	0.002759	0.002713	0.009
4727.120	18.532293	0.001872	0.002483	0.011
4794.553	18.774812	0.006853	0.006452	0.013
4863.941	19.056554	0.005837	0.003726	0.013
4935.363	19.339553	0.007928	0.002462	0.012
5008.938	19.638133	0.005359	0.002394	0.013
5075.157	19.896164	0.000665	0.003825	0.013
5143.135	20.159812	0.002153	0.002934	0.013
5212.993	20.451623	-0.001526	0.001958	0.022
5284.739	20.708035	0.005369	0.005084	0.014
5358.465	21.004088	0.002927	0.000406	0.015
5434.247	21.293578	0.004805	0.001182	0.018
5512.189	21.585659	0.002750	0.003571	0.017
5591.571	21.871333	-0.002629	0.010497	0.066
5674.107	22.189704	-0.004736	0.009859	0.073
5746.794	22.466914	-0.003930	0.009652	0.066
5822.378	22.765496	-0.003993	0.004415	0.031
5898.868	23.041601	-0.003342	0.007476	0.027
5977.385	23.362297	0.002882	0.003516	0.026

A	B	C	D	Δλ (Å)
6058.253	23.666437	-0.008640	-0.000418	0.049
6140.930	23.960718	-0.012851	0.000485	0.053
6225.993	24.253797	0.000309	0.005179	0.019
6313.127	24.549821	0.000396	0.008684	0.024
6402.936	24.877470	0.004497	0.004430	0.024
6495.135	25.194388	0.002021	0.000968	0.018
6589.937	25.500733	-0.004884	0.002764	0.020
6687.268	25.816164	-0.004545	0.002836	0.019
6787.011	26.148175	-0.008249	0.000359	0.057
6889.598	26.454612	0.004830	0.007925	0.025
6977.485	26.769629	0.000637	0.003913	0.020
7067.097	27.088414	0.004600	0.004974	0.029
7159.223	27.450403	0.006491	0.002028	0.018
7253.568	27.833010	0.008206	0.000551	0.015
7350.084	28.193783	0.012243	0.008156	0.011
7449.733	28.597318	0.011064	0.009039	0.020
7552.216	29.030082	0.010674	0.006705	0.013
7657.537	29.460104	0.012234	0.002152	0.027
7765.982	29.877852	0.010485	0.003147	0.030
7877.455	30.324444	0.002001	0.001310	0.015
7992.283	30.750732	0.000950	0.005626	0.020
8110.486	31.205559	-0.001872	0.005153	0.021
8232.227	31.674039	-0.000376	0.002490	0.011
8332.508	32.051572	0.007134	0.003643	0.045
8435.029	32.438447	0.006073	0.006290	0.027
8540.141	32.861226	-0.000622	0.003071	0.049
8647.890	33.295238	0.005924	0.000471	0.028
8758.134	33.728077	0.002790	0.004472	0.021
8871.645	34.186799	0.010132	0.005949	0.039
8987.910	34.644228	0.001605	0.008245	0.014

I. Stability

Because of a very tight time schedule due to the late delivery of the etalon, we have not been able to carry out an extensive set of stability measurements. We did repeat measurements of the peak transmission wavelength at 6100 Å three times over a 6-day period and found an RMS deviation of 0.11 Å, or 1/7th of the 0.79 Å FWHM. The FWHM itself varied by no more than 0.01 Å. The optimum parallelism settings for the three measurements were identical. This level of stability is consistent with our expectations from the other etalons, and more extensive stability measurements will be obtained during commissioning.

J. Discussion

Etalon 1054 exhibits the same bi-modal behavior of the effective gap, with its effect on parallelism, resolution, and free spectral range, that we observed in the other two PFIS etalons. There was no specification on the constancy of effective gap, and the gap is within specification at the specified wavelength of 6500 Å. The effect of the wavelength dependent parallelism setting is an annoyance and will be dealt with in the operating software, but should not degrade the performance of the system. Since a typical wavelength scan for this etalon will be very small compared to the scale over which the parallelism changes, the operating procedure will be to set the parallelism settings to the appropriate values for the center of the scan, and there will be no need to vary the settings over the scan range. We have observed that the parallelism settings are very stable over significant time periods in the laboratory, and will investigate the stability of the parallelism settings in the SALT environment during commissioning. We suspect that they will be very stable, since it is an effect of the physical structure of the coating layers. Thus we expect that we should be able to determine the calibration of the X and Y offset settings as a function of wavelength and not need to re-determine these values each time the FP system is used.

The plate flatness deviates significantly from specification, reaching about $\lambda/50$ rather than the specified the $\lambda/100$. The manufacturer has provided interferograms that indicate that the flatness of the plates met or exceeded the specifications before coating and assembly into the etalon. We have discovered some reports in the literature that document an apparent flatness degradation due to effects in multilayer coatings similar to those employed here. Wavelength gradients in the phase change upon reflection in the coatings can amplify the physical irregularities in the coatings, leading to apparent curvature of the plates. Depending on the details of the coating design (not available to us), this effect can increase or decrease the apparent curvature of the plates, leading to different surface shapes at different wavelengths, as we have observed. If this effect is the source of the observed flatness variation, there is essentially no way to improve the performance of the etalon without stripping the coatings and designing a new coating scheme. Since the coating design is a tradeoff between these effects and the requirement of maintaining a high reflectivity over a wide spectral range, it is not clear that a fully satisfactory solution can be found. Another possible source of the problem insufficient mechanical support of the etalon plates when the etalon is used in a tipped configuration, which could possibly be fixed by redesigning the etalon support system. We will investigate this issue thoroughly during commissioning. The defect finesse produced by these flatness deviations leads to lower spectral resolution and finesse than we had targeted. The spectral resolution is about 65% of the expected value of 12500. We expect that many of the science programs planned to use HR mode will still be successful at these lower resolutions. If it is decided after commissioning tests that higher resolution is required in HR mode, we could explore with the vendor possible modifications of the etalon; a more robust suspension system may be possible, or the gap could be increased to provide the desired resolution (but still with finesse lower than desired).

The transmission of the etalons was not included in the specifications. Our PDR documentation gave a goal of 75 – 80%. The goal is generally met or exceeded in the middle of the etalon's wavelength range, but the transmission is lower, from 40 – 60%, at both shorter and longer wavelengths. At the shorter wavelengths the reduced transmission is probably due to the relatively larger effect of the defect finesse at short wavelengths (a given physical distortion of the plates is a larger number of waves at shorter wavelengths). At the longer wavelengths, our testing procedure may have been flawed, because we did not exclude second order blue light with an appropriate order sorting filter; this contamination would lower the measured transmission. On-sky testing during commissioning observations will provide another measure of the etalon throughput

The wavelength calibration and stability results are in agreement with our expectations based on previous FP systems. We plan on taking calibration exposures at hourly intervals during observations, and it seems that this will provide an adequate measurement of the wavelength drift of the etalon. The actual stability is likely to be heavily dependent on the environmental conditions at the telescope, so we will not be able to determine the required frequency of calibrations until commissioning at SALT.

In summary, although we are disappointed in the resolution and finesse of the etalon, we do not believe that there are any easy ways for the manufacturer to significantly improve the performance in these areas. Since all three etalons suffer from approximately the same relative amount of resolution reduction, the ratio of resolutions provided by the three etalons is approximately what we designed for, and there are thus no large gaps in resolution coverage. We recommend acceptance of the etalon and deployment in PFIS.